



Vacancy surface migration mechanisms in dilute nickel-chromium alloys

Jacob Startt^{a,b}, Chaitanya Deo^{b,c}, Rémi Dingreville^{a,b,*}

^a Center for Integrated Nanotechnologies, Sandia National Laboratories, Albuquerque, NM, 87185, USA

^b George W. Woodruff School of Mechanical Engineering, Georgia Institute of Technology, Atlanta, GA 30332, USA

^c School of Materials Science and Engineering, Georgia Institute of Technology, Atlanta, GA 30332, USA

ARTICLE INFO

Article history:

Received 16 March 2021

Revised 10 May 2021

Accepted 11 May 2021

Available online 26 May 2021

Keywords:

Surface segregation

Atomic migration

Vacancy

Ni-Cr

Density functional theory

ABSTRACT

We investigate the unitary mechanisms related to the surface migration of vacancies in dilute Ni-Cr alloys via first-principle calculations. We survey a complete set of surface and sub-surface migration paths for vacancies near the (100) free surface and calculate the corresponding migration barriers. Our results show that a vacancy migrating towards the free surface will face lower energy barriers to migrate via atomic exchange with a neighboring Cr atom rather than with a Ni atom. Once a vacancy reaches the free surface, it will be trapped there. Our results also reveal that, when a Cr atom sits in the atomic plane just below the free surface, any in-plane vacancy hopping jump that would result in the vacancy sitting on top a subsurface Cr atom is energetically unfavorable. Taken together, these fundamental unitary surface migration mechanisms offer insights into the complex interactions between surface segregation and vacancy migration phenomena in Ni-Cr-based alloys.

© 2021 Acta Materialia Inc. Published by Elsevier Ltd. All rights reserved.

Subtle changes in the surface composition of binary alloys can have significant effects on oxidation and corrosion properties [1,2]. At the atomic scale, these surface changes and corresponding surface dynamics are primarily dictated by both the surface segregation of one of the alloy components and the surface diffusion occurring primarily in the first few atomic planes near the free surface [3]. Regarding surface segregation, some transition-metal-alloy solid solutions display an oscillatory segregation behavior, in which the segregation energy of a solute atom oscillates as a function of depth from the free surface [4–6]. In the case of nickel-chromium (Ni-Cr), this oscillatory behavior cannot be attributed solely to the commonly-accepted lattice relaxation mechanism [6,7] given the similarity in atomic radii between Ni (0.124 nm) and Cr (0.127 nm). Rather, we recently showed that a charge transfer interaction between the Cr atom and the surrounding local Ni lattice also contributes to this oscillatory behavior in Ni-Cr [8]. Regarding surface diffusion, this process can be thought of in terms of the motion of adatoms and vacancies at the free surface via atomic exchange. Ab-initio treatments of vacancy diffusion have largely been focused within the bulk regions of alloys (e.g., Refs. [9–13]) or on metallic oxide surfaces (e.g., Refs. [14–17]). By comparison, the modeling of vacancy energetics near alloy surfaces has been scarce (e.g.,

Refs. [18,19]). While it has been shown that, in bulk Ni-Cr, Cr is the fastest diffusing species in Ni by both vacancy and interstitial diffusion [20,21], the migration mechanisms of Cr and vacancies near a free surface are not as well characterized due to the added complexity introduced by the oscillatory surface segregation behavior. The Ni-Cr system is an important model alloy for Ni-based alloys and austenitic steels. For example, the formation of chromium oxide is important for their corrosion resistance [22,23]. A fundamental understanding of the elementary migration mechanisms of Cr and vacancies near a free surface in Ni are important since they are at the root of more complex surface- and diffusion-driven degradation mechanisms in Ni-Cr-based alloys including Cr depletion or oxide formation for instance. In this letter, we study the unitary mechanisms related to surface migration of vacancies in dilute Ni-Cr alloys near the (100) free surface using density-functional theory (DFT) calculations. We identify a complete set of surface and sub-surface migration paths for a vacancy near this free surface via the climbing image nudged elastic band (CI-NEB) method within the standard DFT formalism, and we calculate the migration barriers for their diffusion. By comparing competing pathways, we can determine the most likely surface migration mechanisms and provide insights into the energetics linking vacancy migration to Cr segregation.

We carried out our DFT simulations using the Vienna Ab-initio Simulation Package (VASP) [24,25]. We treated the electron-ion interactions using the plane-wave basis sets and the projector

* Corresponding author.

E-mail address: rdingre@sandia.gov (R. Dingreville).

augmented wave (PAW) method [26,27], and we described the exchange-correlation energy functional with the Perdew-Burke-Ernzerhof (PBE) [28] formulation of the generalized gradient approximation (GGA). In all the simulations, we treated the $\text{Ni}(3d^8 4s^2)$ and $\text{Cr}(3d^5 4s^1)$ valence electrons explicitly, while all other electrons were treated within the frozen core of the pseudopotentials. We used a 400-eV plane-wave cutoff for the plane-wave expansion of the wavefunctions, while minimization of the electronic wavefunction was achieved with an energy convergence below 10^{-6} eV. Ionic minimization was reached when forces on all atoms fell below 0.02 eV/Å. For all of our calculations, we set the partial orbital occupancies according to the smearing method of Methfessel-Paxton of order one [29] with a smearing width of 0.2 eV. In dilute Ni-Cr alloys, Cr anti-ferromagnetically couples to Ni [30–32]. Therefore we considered spin-polarization effects in our simulations by initializing the Cr spin anti-ferromagnetically to the spin of the nearby Ni atoms. For all migration paths modeled, we found that this anti-ferromagnetic coupling remained throughout the entirety of each migration jump. In some cases, it was possible for the spin of the Cr atom to flip, aligning ferromagnetically with the Ni. However, this was always accompanied by a sharp increase in the total energy, indicating a metastable ordering. For all the configurations tested, we calculated the minimum-energy paths for various migration pathways using a NEB-transition-state-search method. The transition state search for the minimum energy path between each initial and final jump configuration was performed using the CI-NEB method [33–35]. We found the ground states of the initial and final configurations first through standard DFT-relaxation methods, and then determined an approximate path between them through linear interpolation. This path was then populated with five climbing images. A spring constant of 5 eV/Å² ensured that the center image was pushed to the top the migration barrier.

As illustrated in Fig. 1, we modeled the Ni(100) surface by constructing a seven-layer surface slab containing 175 Ni atoms, with a ABA'B' stacking sequence and 25 atoms per atomic plane. The AB notation refers to the stacking of face centered cubic (FCC) atomic planes in the [001] surface normal direction. B atomic planes are offset from A planes by $1/2 a_0$ [100], with a_0 being the Ni lattice constant. The A' and B' notation indicates the second consecutive set of A and B atomic planes from the surface (i.e., the third and fourth atomic planes). We fixed the bottom-

two atomic planes to enforce bulk-like behavior at the bottom of the slab (i.e., atoms are constrained to maintain a desired lattice constant, and are not subject to free-surface relaxation). We fixed the vacuum thickness separating the periodic slabs to 12 Å above the free surface to avoid interactions across the boundary of the simulation cell. We carried out all of our calculations using a $6 \times 6 \times 1$ k-point mesh which yielded sufficiently accurate and converged results. We selected the (100) surface orientation as an exemplar, isotropic surface with a low Miller index. As a benchmark, we calculated the surface energy for this slab by doubling the number of layers and allowing both sides to fully relax. We found a surface energy of 2.24 J/m² which agrees reasonably well with the measured experimental value of 2.45 J/m² [36]. For calculations containing a vacancy, we first inserted the vacancy into the fourth atomic plane by removing a Ni atom near the center of that atomic plane. From this configuration, we performed calculations allowing atomic relaxation of the vacancy for the top four nickel atomic planes, considering only unique jumps: out-of-plane (upward/downward) and in-plane (sideways). For this surface orientation, the in-plane directions consist of the [110], $\bar{1}\bar{1}0$, and $[1\bar{1}0]$ directions, while the out-of-plane directions consist of the [011], $\bar{0}\bar{1}1$, $[01\bar{1}]$, $[0\bar{1}1]$, $[101]$, $[10\bar{1}]$, $[\bar{1}01]$, $[\bar{1}0\bar{1}]$ directions. The possible pathways for vacancy migration are depicted in Fig. 1.

We first calculated the migration energy barriers of a single vacancy through a pure Ni(100) surface with no Cr. The minimum-energy paths for the various migration pathways considering different atomic planes are presented in Fig. 2. The solid curves represent the upward/out-of-plane migration paths of the vacancy. As the vacancy migrates upward, the final position of each migration becomes the starting position of the next consecutive upward jump. As such, the energy barriers can be connected to form a continuous path from the near-bulk B' atomic plane to the surface A atomic plane. The dashed lines represent the minimum-energy paths for in-plane jumps serving as competing pathways to the out-of-plane migration paths. Our results show that, in the near-bulk region of the slab (i.e., B' atomic plane), the upward and in-plane energy paths are nearly identical. As tabulated in Table 1, the migration-barrier heights of 1.063 eV (upward B' → A') and 1.093 eV (in-plane B' → B') are in agreement with existing experimental and computational bulk values [21,37]. These results indicate that the effect of the surface on the upward and in-plane migration pathways of a vacancy is mostly negligible in these deeper sub-surface atomic planes and so they can be considered bulk-like. However, as the vacancy moves upward (i.e., towards A', B, or A atomic planes), the surface gradually alters the migration energetics. In this case, the upward out-of-plane migration becomes favored over the in-plane migration. As seen in Fig. 2 and in Table 1, this action is governed not only by a decrease in the out-of-plane barriers relative to the in-plane barriers in the near surface atomic planes, but also by a decrease in the ground-state energy of the final position in the first atomic plane (i.e., the vacancy is most stable in this atomic plane). In addition, our results point out that downward migrations are highly unfavored in the pure Ni(100) surface. As shown in Table 1, the in-plane migration barrier for a vacancy in the top atomic plane, A → A, is 0.559 eV, while the backward migration energy, A → B, corresponding to a vacancy migrating back down into the subsurface, is nearly three times as much at 1.501 eV. From these calculations, we deduce that, should a vacancy make its way into the vicinity of the free surface (i.e., third atomic plane or above), it will likely be captured by the surface, from which it is expected to remain trapped and diffuse in-plane from that point on.

We next turn our attention on how the vacancy-migration behavior changes when Cr is present in the vicinity of the surface (i.e., within the top three atomic planes). We considered two con-

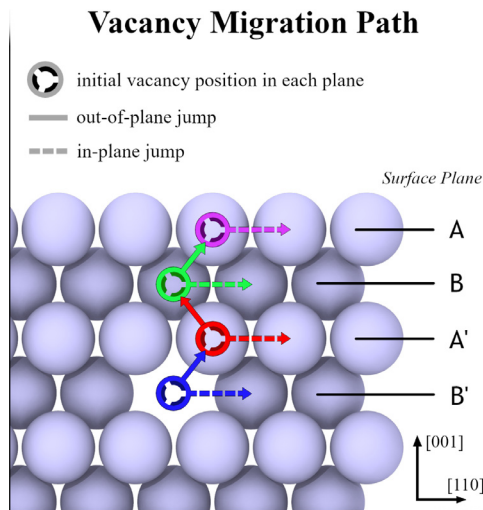


Fig. 1. Migration path of the vacancy in the pure Ni (100) surface. The vacancy starts in plane B' and can jump either in-plane (dashed arrow) or out-of-plane (solid arrow). Out-of-plane jumps in the up or down direction (relative to the surface) are considered equivalent and so are only explicitly modeled in the up direction.

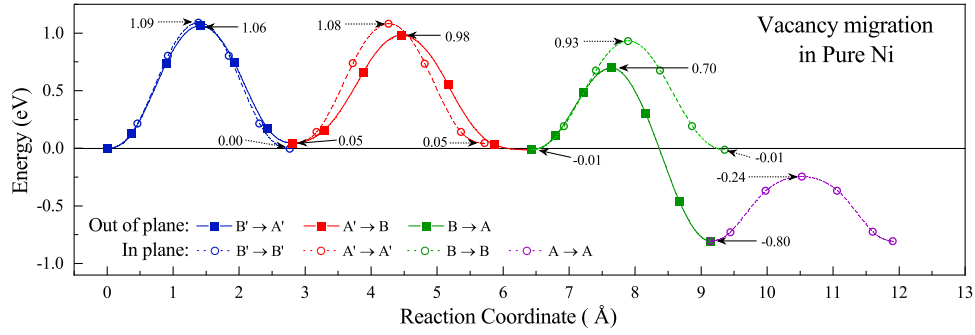


Fig. 2. CI-NEB energy barriers for the migration of a single vacancy through a Ni(100) surface. The solid curves represent the minimum energy path for the vacancy as it moves out-of-plane. The dashed curves (open circles) depict the minimum energy path corresponding to the competing in-plane jumps. The reaction coordinate represents only the distance travelled by the vacancy along the reaction path and should not be taken as the exact distance from the surface, particularly in the case of the in-plane jumps.

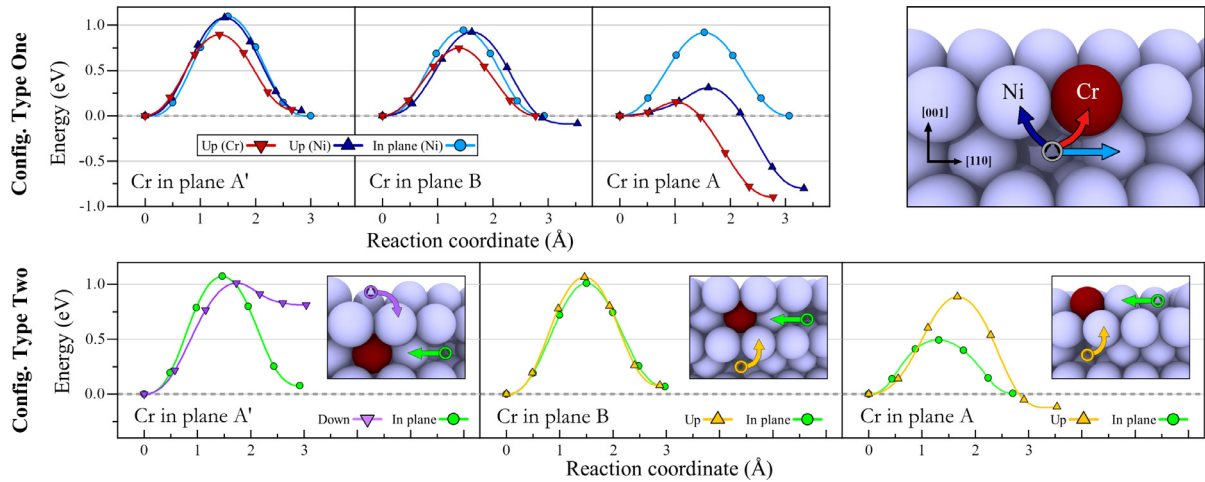


Fig. 3. Migration energy barriers calculated for vacancy jumps in the vicinity of a Cr atom near the surface. The top row depicts the relative competition for the vacancy, already adjacent to the Cr, to swap places with the Cr atom or other nearby Ni atoms. The bottom row shows migration barriers for the vacancy, initially not adjacent to the Cr atom, to hop into a site directly adjacent to the Cr atom.

Table 1

Energy barriers (in eV) for a single vacancy near a Ni(100) surface as a function of the pathway. Columns: initial plane of vacancy, rows: final plane of vacancy. Diagonal values (e.g., $B' \rightarrow B'$, $A' \rightarrow A'$, ...) represent in-plane migration barriers, off-diagonal values (e.g., $B' \rightarrow A'$, $B \rightarrow A$, ...) represent upward/downward migration barriers. The first value shown in each cell (in parenthesis) represent energy barriers for the pure Ni system and correspond to pathways shown in Fig. 2. The remaining values are for the system containing one Cr atom and correspond to the pathways shown in the first row of Fig. 3. In this latter case, for the out-of-plane jumps (off-diagonal values) the vacancy can exchange places with either a Cr (red paths in Fig. 3) or a Ni atom (dark blue paths in Fig. 3). For the in-plane jumps, the vacancy can only exchange positions with a Ni atom (light blue paths in Fig. 3). The energy barriers for these separate Cr and Ni paths are both reported in the off-diagonal elements as $\langle \text{Cr} \rangle / \langle \text{Ni} \rangle$. For instance, the upward migration of a vacancy moving from the B atomic plane to the A atomic plane has an energy barrier of 0.151 eV to migrate via the Cr atom, or 0.310 eV via the Ni atom.

		Initial			
		B'	A'	B	A
Final	A	-	-	(0.710)/0.151/0.310	(0.559)
	B	-	(0.936)/0.578/0.748	(0.946)/0.918	(1.501)/1.049/1.11
	A'	(1.063)/0.694/0.896	(1.035)/0.945	(0.994)/0.925/1.013	-
	B'	(1.093)/1.098	(1.063)/0.694/0.896	-	-

figurations. In a first series of calculations (top row in Fig. 3), we examined the configuration where a vacancy can swap position with either a Cr (red path) or Ni (dark and light blue paths) atom. In this case the vacancy is adjacent to the Cr atom (i.e., the Cr atom is under-coordinated). In the second series of calculations (bottom row in Fig. 3), we looked into the configuration where a vacancy hops towards a Cr atom by exchanging position with one of the

Cr first nearest-neighbor Ni atoms. In this case, the vacancy is not initially adjacent to the Cr atom, and the Cr atom is fully coordinated. For both sets of calculations, we considered both in-plane and out-of-plane motions for the vacancy. The migration-energy barriers for both sets of calculations are listed in Table 1. Concerning the first set, our results show that, regardless of where the Cr atom sits with respect to the free surface, the vacancy will ener-

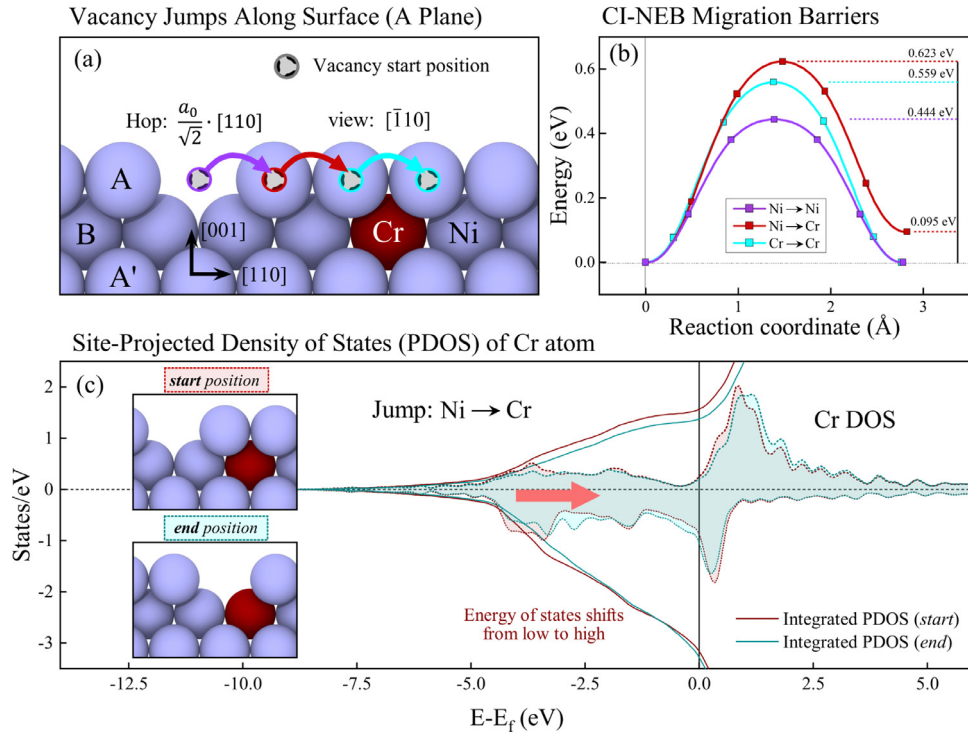


Fig. 4. Chromium shielding by vacancy migration in the surface layer. (a) The vacancy is migrating in the [110] direction through the surface A atomic plane. (b) Migration barriers as the vacancy migrates over Ni and Cr atoms in the subsurface B atomic plane. The energy barrier to migrate over a Ni atom is 0.18 eV lower than the barrier required to migrate over an isolated Cr atom. (c) Site projected density of states (PDOS).

getically favor an upward hop via a swap with the Cr atom rather than with a Ni atom due to a lower migration barrier. This atomic-exchange mechanism is especially favored when the Cr atom sits in the surface atomic plane A, promoting the Cr atom to move within the subsurface B atomic plane. This observation concurs with the oscillatory-segregation behavior for Cr which preferably sits in the second atomic plane. Additionally, the migration barriers calculated for the near-bulk region (*i.e.*, when the Cr atom sits in the B' atomic plane) for both Ni and Cr atoms match well with previously calculated bulk values [21,37]. Interestingly, since the Ni migration barrier corresponding to a migration back down into the subsurface is larger than the Cr barrier (see values list in Table 1), the migration of the vacancy down into the subsurface is slightly more favored to occur via the Cr atom than the Ni atom. However, this mechanism is deemed unlikely given the steep migration barrier for a backward vacancy migration as compared to an in-plane migration. Our second set of calculations (bottom two rows in Fig 3) shows that, regardless of where the Cr atom sits with respect to the free surface, the vacancy will energetically favor in-plane or out-of-plane in order to avoid the under-coordinated configuration for the Cr atom. This is particularly true at the surface, where the contribution of the Cr atom relative to Ni atom on the surface energy causes Cr segregation to the surface atomic plane to become unfavorable [6,32,38].

We have shown in Figs. 2 and 3 that once vacancies migrate to the surface atomic plane A, they become trapped there facing a steep energy barrier to migrate back down. As seen in Fig. 4, our results show that once in the surface atomic plane, the vacancy shields the Cr atoms in the second atomic plane from becoming exposed to the free surface. As illustrated in Fig. 4(a), the vacancy migration path within the surface atomic plane can be characterized by the type of atoms sitting just below it in the second atomic plane. We modeled A→A in-plane vacancy migration over both subsurface Ni and Cr atoms (jumps labeled as Ni→Ni,

Ni→Cr and Cr→Cr, respectively). We show the NEB migration barriers for each of these jumps in Fig. 4(b). The barrier for Ni→Ni is the lowest at 0.444 eV, while the barriers for Ni→Cr and Cr→Cr representing jumps to a position above a Cr atom are appreciably higher at 0.623 eV for Ni→Cr and 0.559 eV for Cr→Cr. This energy penalty is partially due to the fact that the ground-state energy of the exposed Cr atom in the second atomic plane (*i.e.*, the end position of Ni→Cr) is higher than the ground-state energy of the initial position in which the Cr is fully surrounded by Ni atoms. The site-projected density of states (PDOS) in Fig. 4(c) shows how the energy of the occupied states around the Cr atom shifts in response to the vacancy moving to a position directly above the Cr atom (*i.e.*, Ni→Cr in Fig. 4(a)). There is a clear shift in the DOS from low (red DOS) to high energy (teal DOS) as the vacancy moves above the Cr atom, causing it to become exposed to vacuum and therefore under-coordinated. This shift is indicated in the integrated PDOS (solid lines) of the spin-up and spin-down states at each position by the greater density of states at lower energies. This shift reveals that it is more likely that vacancies migrating through the surface will be energetically penalized for migration jumps that take them directly over Cr atoms in the second atomic plane. Thus, Cr atoms in the B atomic plane are less likely to become exposed to the free surface than Ni atoms when there are high fluxes of vacancies at the surface.

These results offer insights into the interactions between surface segregation and vacancy migration phenomena near (100) surfaces in dilute Ni-Cr system. We show that a vacancy migrating towards the free surface will face lower energy barriers to migrate via atomic exchange with a neighboring Cr atom rather than with a Ni atom. This result suggests that diffusion of vacancies to the surface should result in a backward flux of Cr in the atomic plane just below the surface. Furthermore, our NEB results reveal that, when a Cr atom sits in the atomic plane just below the free surface, any in-plane vacancy migration jump that would result in the

vacancy sitting on top a subsurface Cr atom is an energetically unfavorable jump.

Declaration of Competing Interest

The authors declare that they have no known competing financial interests or personal relationships that could have appeared to influence the work reported in this paper.

Acknowledgements

The authors acknowledge J. Tranchida and M.A. Wood from Sandia National Laboratories for comments and review of this work. This work was performed, in part, at the Center for Integrated Nanotechnologies, an Office of Science User Facility operated for the U.S. Department of Energy. Sandia National Laboratories is a multi-mission laboratory managed and operated by National Technology and Engineering Solutions of Sandia, LLC., a wholly owned subsidiary of Honeywell International, Inc., for the U.S. Department of Energy's National Nuclear Security Administration under contract DE-NA0003525. The views expressed in this article do not necessarily represent the views of the U.S. Department of Energy or the United States Government.

References

- [1] J.A. Rodriguez, Surf. Sci. Rep. 24 (7) (1996) 223–287, doi:[10.1016/0167-5729\(96\)00004-0](https://doi.org/10.1016/0167-5729(96)00004-0).
- [2] A.V. Ruban, H.L. Skriver, J.K. Nørskov, Phys. Rev. B 59 (24) (1999) 15990–16000, doi:[10.1103/PhysRevB.59.15990](https://doi.org/10.1103/PhysRevB.59.15990).
- [3] H.-C. Jeong, E.D. Williams, Surf. Sci. Rep. 34 (6–8) (1999) 171–294, doi:[10.1016/S0167-5729\(98\)00010-7](https://doi.org/10.1016/S0167-5729(98)00010-7).
- [4] J. Tersoff, Phys. Rev. B 42 (17) (1990) 10965–10968, doi:[10.1103/PhysRevB.42.10965](https://doi.org/10.1103/PhysRevB.42.10965).
- [5] D.M. Ren, J.H. Qin, J.B. Wang, T.T. Tsong, Phys. Rev. B 47 (7) (1993) 3944–3946, doi:[10.1103/PhysRevB.47.3944](https://doi.org/10.1103/PhysRevB.47.3944).
- [6] Y. Yu, W. Xiao, J. Wang, L. Wang, Phys. Chem. Chem. Phys. 18 (38) (2016) 26616–26622, doi:[10.1039/c6cp02983c](https://doi.org/10.1039/c6cp02983c).
- [7] S. Helfensteyn, J. Luyten, L. Feyaerts, C. Creemers, Appl. Surf. Sci. 212 (2003) 844–849, doi:[10.1016/S0169-4332\(03\)00088-6](https://doi.org/10.1016/S0169-4332(03)00088-6).
- [8] J. Startt, R. Dingreville, S. Raiman, C. Deo, Acta Mater., under review (2021).
- [9] K. Carling, G. Wahnström, T.R. Mattsson, A.E. Mattsson, N. Sandberg, G. Grimvall, Phys. Rev. Lett. 85 (18) (2000) 3862–3865, doi:[10.1103/PhysRevLett.85.3862](https://doi.org/10.1103/PhysRevLett.85.3862).
- [10] E.H. Megchiche, S. Pérusin, J.-C. Barthelat, C. Mijoule, Phys. Rev. B 74 (6) (2006) 064111.
- [11] M. Mantina, Y. Wang, R. Arroyave, L.Q. Chen, Z.K. Liu, C. Wolverton, Phys. Rev. Lett. 100 (21) (2008) 215901, doi:[10.1103/PhysRevLett.100.215901](https://doi.org/10.1103/PhysRevLett.100.215901).
- [12] S. Choudhury, L. Barnard, J.D. Tucker, T.R. Allen, B.D. Wirth, M. Asta, D. Morgan, J. Nucl. Mater. 411 (1) (2011) 1–14, doi:[10.1016/j.jnucmat.2010.12.231](https://doi.org/10.1016/j.jnucmat.2010.12.231).
- [13] J.-H. Ke, G.A. Young, J.D. Tucker, Acta Mater. 172 (2019) 30–43, doi:[10.1016/j.actamat.2019.04.036](https://doi.org/10.1016/j.actamat.2019.04.036).
- [14] E. Florez, P. Fuentealba, F. Mondragón, Catal. Today 133–135 (2008) 216–222, doi:[10.1016/j.cattod.2007.12.087](https://doi.org/10.1016/j.cattod.2007.12.087).
- [15] J. Jeon, B.D. Yu, S. Hyun, Curr. Appl. Phys. 15 (6) (2015) 679–682, doi:[10.1016/j.cap.2015.03.003](https://doi.org/10.1016/j.cap.2015.03.003).
- [16] R. Panta, V. Ruangpornvisuti, Int. J. Hydrog. Energy 42 (30) (2017) 19106–19113, doi:[10.1016/j.ijhydene.2017.04.251](https://doi.org/10.1016/j.ijhydene.2017.04.251).
- [17] D. Tian, C. Zeng, H. Wang, X. Cheng, Y. Zheng, C. Xiang, Y. Wei, K. Li, X. Zhu, Appl. Surf. Sci. 416 (2017) 547–564, doi:[10.1016/j.apsusc.2017.04.028](https://doi.org/10.1016/j.apsusc.2017.04.028).
- [18] R.P. Kauffman, A.M. Rappe, Phys. Rev. B 67 (8) (2003) 085403, doi:[10.1103/PhysRevB.67.085403](https://doi.org/10.1103/PhysRevB.67.085403).
- [19] A.R. Akbarzadeh, Z.Z. Chen, N. Kioussis, Phys. Rev. B 79 (19) (2009) 195404, doi:[10.1103/PhysRevB.79.195404](https://doi.org/10.1103/PhysRevB.79.195404).
- [20] J.D. Tucker, R. Najafabadi, T.R. Allen, D. Morgan, J. Nucl. Mater. 405 (3) (2010) 216–234, doi:[10.1016/j.jnucmat.2010.08.003](https://doi.org/10.1016/j.jnucmat.2010.08.003).
- [21] S. Zhao, G.M. Stocks, Y. Zhang, Phys. Chem. Chem. Phys. 18 (34) (2016) 24043–24056, doi:[10.1039/C6CP05161H](https://doi.org/10.1039/C6CP05161H).
- [22] C.-C. Shih, C.-M. Shih, Y.-Y. Su, L.H.J. Su, M.-S. Chang, S.J. Lin, Corr. Sci. 46 (2) (2004) 427–441, doi:[10.1116/1.580010](https://doi.org/10.1116/1.580010).
- [23] T.S. Sidhu, S. Prakash, R.D. Agrawal, Scripta Mater. 55 (2) (2006) 179–182, doi:[10.1016/j.scriptamat.2006.03.054](https://doi.org/10.1016/j.scriptamat.2006.03.054).
- [24] G. Kresse, J. Hafner, Phys. Rev. B 47 (1) (1993) 558–561, doi:[10.1016/0022-3093\(95\)00355-X](https://doi.org/10.1016/0022-3093(95)00355-X).
- [25] G. Kresse, J. Furthmüller, Comput. Mater. Sci. 6 (1) (1996) 15–50, doi:[10.1016/0927-0256\(96\)00008-0](https://doi.org/10.1016/0927-0256(96)00008-0).
- [26] P.E. Blochl, Phys. Rev. B 50 (24) (1994) 17979, doi:[10.1103/PhysRevB.50.17953](https://doi.org/10.1103/PhysRevB.50.17953).
- [27] G. Kresse, D. Joubert, Phys. Rev. B 59 (3) (1999) 1758–1775, doi:[10.1103/PhysRevB.59.1758](https://doi.org/10.1103/PhysRevB.59.1758).
- [28] J.P. Perdew, K. Burke, M. Ernzerhof, Phys. Rev. Lett. 77 (18) (1996) 3865–3868, doi:[10.1103/PhysRevLett.77.3865](https://doi.org/10.1103/PhysRevLett.77.3865).
- [29] M. Methfessel, A.T. Paxton, Phys. Rev. B 40 (6) (1989) 3616–3621, doi:[10.1103/PhysRevB.40.3616](https://doi.org/10.1103/PhysRevB.40.3616).
- [30] M.J. Besnus, Y. Gottehrer, G. Munschy, Phys. Status Solidi B 49 (2) (1972) 597–607, doi:[10.1002/pssb.2220490222](https://doi.org/10.1002/pssb.2220490222).
- [31] J.R. Thompson, A. Goyal, D.K. Christen, D.M. Kroeger, Physica C Supercond. 370 (3) (2002) 169–176, doi:[10.1016/S0921-4534\(01\)00937-6](https://doi.org/10.1016/S0921-4534(01)00937-6).
- [32] M. Aldén, H.L. Skriver, S. Mirbt, B. Johansson, Surf. Sci. 1–2 (315) (1994) 157–172, doi:[10.1016/0039-6028\(94\)90551-7](https://doi.org/10.1016/0039-6028(94)90551-7).
- [33] D. Sheppard, R. Terrell, G. Henkelman, J. Chem. Phys. 128 (13) (2008) 134106, doi:[10.1063/1.2841941](https://doi.org/10.1063/1.2841941).
- [34] G. Henkelman, B.P. Uberuaga, H. Jónsson, J. Chem. Phys. 113 (22) (2000) 9901–9904, doi:[10.1063/1.1329672](https://doi.org/10.1063/1.1329672).
- [35] G. Henkelman, H. Jónsson, J. Chem. Phys. 113 (22) (2000) 9978–9985, doi:[10.1063/1.1323224](https://doi.org/10.1063/1.1323224).
- [36] F.R.d. Boer, W.C.M. Mattens, R. Boom, A.R. Miedema, A.K. Niessen, Cohesion in Metals, North-Holland, Netherlands, 1988.
- [37] D. Chakraborty, D.S. Aidhy, J. Alloys Compd. 725 (2017) 449–460, doi:[10.1016/j.jallcom.2017.07.140](https://doi.org/10.1016/j.jallcom.2017.07.140).
- [38] S.-P. Jeng, P.H. Holloway, C.D. Batich, Surf. Sci. Lett. 193 (1988) L63–L68, doi:[10.1016/0039-6028\(88\)90437-2](https://doi.org/10.1016/0039-6028(88)90437-2).